Proceedings of the
Annual Stability Conference
Structural Stability Research Council
Toronto, Canada, March 25-28, 2014

Stability of continuous steel column members at elevated temperatures

Corbin St. Aubin[1] and Amit H. Varma[2]

Abstract
AISC 360-10 prescribes design guidelines to determine the strength of steel columns at elevated temperatures. These guidelines are only applicable to columns in building structures with simply supported end conditions. Surrounding members may restrain the column from undergoing axial and rotational deformations due to elevated temperatures. Disregarding the effects of rotational restraints to design the column for simply supported end conditions becomes increasingly conservative. The presence of surrounding columns unaffected by fire can have a significant stabilizing effect on the heated column(s). Eurocode-3 (EN 1993-1-2, 2005) attempts to account for these restraints and recommends arbitrarily the reduction of column unbraced length to 50% for columns that are continuous at both ends and 70% for columns that are continuous at one end. Finite element modeling software has been used to quantify the effect of rotational restraint, but there have been very few experimental tests to supplement these results. Parametric studies conducted by the authors have shown that rotational restraints can significantly reduce the effective length with increase in column temperature. A series of laboratory-scale tests were conducted at Purdue University to investigate the realistic effects of rotational restraints created by continuous columns. Steady-state thermal tests have been completed on W5X16 and W4X13 column specimens that were continuous at both ends. Tests were conducted in the temperature range of 350°C to 600°C. The results of these tests as well as design recommendations are discussed in this paper.

Keywords: Fire, steel column, rotational restraint

[1] Graduate Research Assistant, Purdue University, Bowen Laboratory, 1040 South River Road, West Lafayette, IN 47907, Email: cstaubin@purdue.edu
[2] Associate Professor, School of Civil and Environmental Engineering, Purdue University, 550 Stadium Mall Drive, West Lafayette, IN 47907, Email: ahvarma@purdue.edu

1. Introduction

Current Eurocode design methodologies for compressive members in a braced frame system assume a reduced buckling length of 0.5 times the column height for intermediate stories and 0.7 times the column height for the top story as seen in Figure 1. These assumptions are based on a case in which there is a compartment fire and the structural elements outside of the compartment remain at ambient temperature. The Eurocode idealized length reduction factors are assuming that the surrounding elements provide fixed conditions when in reality the condition is neither fixed nor hinged but somewhere in between.

Ali and O'Connor (2001) tested ten half-scale specimens with varied rotational restraints and axial loadings. The testing considered two different levels of rotational restraint. The rotational restraint was applied to the system by means of steel plates at either end of the column. The steel plates in all tests were 200 X 750 mm; the plate thickness were 10 mm to 40 mm for the low restraint and high restraint respectively. The tests illustrated that the addition of rotational restraint can significantly increase the failure temperature of the column under the same axial load. Also, the column effective length was calculated by means of the geometric data obtained from the failed specimen. The effective length of the ten specimen were found to be between 0.52L and 0.65L where L is the column height. The results of these tests show that rotational restraints at either end of a column will reduce its effective buckling length and the assumption of 0.5L may be unconservative because real conditions will not reflect a true fixed-fixed response.

Agarwal and Varma (2011), modeled the thermal and structural response of continuous columns. The modeling included parametric studies on W8X35, W12X58, W14X90 and W14X159 shapes which are commonly used in steel construction. The study investigated wide flange shapes with three different boundary conditions: simply supported, continuous at one end and continuous at both ends. In addition to boundary conditions, slenderness and axial loads were varied as part of the study. The study concluded that the failure temperature is greater for a column continuous at one end than a simply supported column, and the failure temperature of a column continuous at both ends is greater than the two previous conditions. The empirical data from the parametric study generated an equation to calculate the effective slenderness (λ_{eff}) of a column continuous at one end and continuous at both ends. Equations 1-3 illustrate this behavior.

$$\lambda_{eff} = \lambda \qquad if\ \lambda \leq 10.5 \tag{1}$$

$$\lambda_{eff} = \left(1 - \frac{T}{2000}\right)\lambda - \frac{35}{2000}T \geq 10.5 \qquad if\ \lambda > 10.5, and\ continuous\ at\ both\ ends \tag{2}$$

$$\lambda_{eff} = \left(1 - \frac{T}{4000}\right)\lambda - \frac{35}{4000}T \geq 10.5 \qquad if\ \lambda > 10.5, and\ continuous\ at\ both\ ends \tag{3}$$

Where λ is the governing slenderness of the column and T is the temperature of the intermediate column in ^{o}C. The effective slenderness calculation was found to offer good agreement in calculating column capacities when used with AISC-360 Equation A-4-2 for compression members at elevated temperatures. This same set of equations can be converted to Fahrenheit to better accommodate US standards.

Figure 2 shows the relationship between the slenderness of a continuous column and the equivalent simply supported column. This figure shows that effective slenderness decreases with increasing

temperature. This figure also shows that the equation is discontinuous due to a minimum slenderness of 10.5 at elevated temperatures.

2. Research Significance

The objectives of this research are to provide experimental results pertaining to the effective slenderness ratio of a continuous column. The tests are meant to simulate a column continuous over three stories where a compartment fire occurs in the intermediate story. The purpose of this is to determine the validity of the proposed equation in calculating effective slenderness for use in determining the critical buckling load of a column that is part of a steel framing system. The results of such tests can also be used to verify existing finite element models and develop a verified approach to calculate slenderness reduction.

The experimental program was developed based on a series of parametric studies performed by Agarwal and Varma (2011), in which the author notes the effects of axial load, slenderness ratio and temperature on the stability of continuous steel columns. The column at elevated temperature was assumed to have uniform thermal distribution through the section considering thermal gradients only along the length of the continuous columns (from column to column). Continuous columns with surrounding cooler members have shown to greatly improve the axial load capacity of the heated column. The research also indicated that continuous columns have no effect on the ambient load capacity of columns as each column are equally close to the respective buckling limit state. The effect of rotational restraint on a partially heated continuous column can be easily implemented by a reduction in slenderness. The research consisted of two cases:

CASE 1: Simply supported column with a cool column on one end. The column failure takes place in the heated span. The load carrying capacity is higher at elevated temperatures relative to a single simply supported column. Also, in a realistic fire scenario, the continuous column will fail at a higher temperature than a single column.

CASE 2: Simply supported continuous column consisting of three column spans. In this case, the heated column is located in the center span and also buckles first. However, columns continuous at both ends will fail at higher temperatures than a column continuous at one end. Also, this effect is more apparent for columns with greater slenderness. In both cases it is assumed that the adjoining column section has the same cross section and slenderness value.

This paper focuses on the second case where the column at elevated temperature is continuous at both ends. A total of six tests were completed on W5X16 and W4X13 sections with a slenderness ratio (λ) equal to 38 and 48 respectively. The tests were conducted at steady-state temperatures of 350^{o}C, 500^{o}C and 600^{o}C. Comparisons with current models as well as the proposed design equation from Agarwal and Varma are reviewed.

3. Test Setup and Instrumentation

The testing was completed using a tension test frame designed and discussed by Choe (2011). Two 4 inch diameter tension rods react against the axially loaded column in the center of the frame in Figure 3. Two reaction beams are located at either end of the setup. The load is introduced by a single hydraulic actuator at the top reaction beam. The load is transferred to the column by half cylindrical frictionless bearings. Heat is applied to the system by two ceramic fiber heaters. The

heaters were placed one inch from the steel surface and insulated to capture the radiant heat. The heaters are controlled by a series of proportional-integral-derivative (PID) controllers that utilize feedback from thermocouple measurements to achieve a desired set-point.

Internal supports are located at 1/3 and 2/3 of the overall specimen length. Each support has four rollers to prevent lateral and out of plane displacement while allowing axial displacements and rotations. Each specimen was a total of 12 ft long, braced at 4 ft points along the length.

K Type thermocouples (wire diameter = 0.81mm) were used to measure steel surface temperatures across the section. 29 thermocouples were located at five separate sections to evaluate the thermal gradient along the length of the column as well as section temperatures. Two thermocouples were used as feedback into the controller box located at the center of the heaters. High temperature strain gages (5mm gage length) were placed at mid-height of the intermediate column as well as one inch outside the interior supports. The mid-height gages were utilized prior to heating to confirm the column was concentrically loaded. Figure 4 presents the thermocouple layout as well as the locations where rotational and linear displacements were measured. Rotational displacements were measured at both internal supports outside the heated zone as well as on both half-cylindrical supports located at the column ends. Lateral displacements were measured at mid-height of each of the three column sections.

4. Boundary Conditions

The column was bounded at the extreme ends by half cylindrical steel bearings greased prior to loading. The bearing allows for free rotation in the direction of the minor axis. Internal supports provide bracing in both major and minor axis by means of steel pin-rollers. The rollers prevented displacement in the braced directions while allowing free deformation axially and rotationally. The unbraced length of all continuous columns was 4 ft prior to loading. A top view of the test setup can be seen in Figure 3.

5. Experimental Procedure

The experimental procedure follows that of a steady-state thermal test in which the temperature is maintained at a set-point for the duration of the test and the axial load is increased monotonically until failure. Before testing, the column is loaded to approximately 10% of the critical buckling load to determine load concentricity. This is repeated to ensure there is no eccentricity present in the system. The column is loaded to 10 kip to ensure the column is seated properly in its bearings and that the internal roller supports are in contact with the specimen. Radiant heat is applied to the center span at a constant rate of 7^{o}C/min until reaching a predefined target temperature at which point the target temperature is maintained constant for the final duration of the test. Axial load is then increased quasi-statically in 5 kip increments until column failure. Column failure was typically observed when runaway deflection occurs. Throughout the test, axial load, axial displacement, lateral displacement, rotation and steel surface temperatures were measured.

6. Test Matrix

A total of six continuous column specimens were tested. Two of the six specimens were W5X16 while the remaining four were W4X13. The slenderness ratio of the W5X16 specimens were 68 and 38 and column buckling occurred followed by local flange distortion. Four W4X13 specimens were tested at varied temperatures with a slenderness ratio of 48. Due to limitations of the test frame, only one slenderness ratio was tested for the W4X13 columns. Table 1 shows the specimen, section, slenderness and temperature at which the columns were tested.

Table 1. Continuous column test matrix

Specimen[1]	Shape	KL/r	Temperature (^oC)
TC-SP1	W5X16	68	500
TC-SP2	W5X16	38	500
TC-SP3	W4X13	48	500
TC-SP4	W4X13	48	600
TC-SP5	W4X13	48	600
TC-SP6	W4X13	48	350

1. Three column – specimen number

7. Experimental Results

Results of the continuous column testing indicated that surrounding cooler members can have a substantial effect on the axial load capacity of a column member. In all tests, the heated column buckled before the surrounding columns, and in most cases, the heated column had larger rotations and lateral displacements than the surrounding columns. Flexural buckling in the minor axis was the failure mode in all tests except for TC-SP1 which buckled in the major axis for reasons explained below. Ambient temperatures for all tests ranged from 14^{o}C to 30 ^{o}C.

7.1 TC-SP1 - W5X16

TC-SP1 was braced at the internal supports only in the direction of the minor axis by means of rollers. The specimen was loaded monotonically in three cycles. The cycles corresponded roughly to 1/4 P_{cr}, 1/2 P_{cr} and failure. The middle column was heated at a rate of 7^{o}C/min for 67 minutes at which time the temperature was maintained at 500^{o}C inside the heated zone. The time-temperature response of the steel can be seen in Figure 5. The external columns were heated from an ambient temperature of 24 ^{o}C to 48^{o}C through conduction. This change in temperature is considered negligible. The column failed in major axis buckling at an axial load of 160 kips because of inadequate restraints for major axis buckling at the internal supports with slenderness equal to 68.

7.2 TC-SP2 – W5X16

TC-SP2 was subject to the same loading scheme as TC-SP1, however the internal supports prevented displacement in both major axis and minor axis. The mechanical loading of the column specimen can be seen in Figure 6. The loading was increased at a rate of 3 kips/min. The heated column lateral displacement begins to displace in the upward direction (negative) due to the steel expansion under a stabilizing load of 10 kips. As the load increases, the displacement increases linearly before final buckling failure occurs (the structural response of TC-SP2 can be seen in

Figure 7). The lateral displacement of the central column is greater than that of either of the surrounding columns. This is significant because it not only shows that buckling was initiated in the heated column, but also that the external columns responded to the central column failure by deflecting in the opposing direction. The action provides the restraining moment at the internal supports that increases the critical buckling load on the column. This is attributed to the larger displacements recorded in the heated column. The column failed at a maximum axial load of 195.5 kips by flexural buckling in the minor axis followed by local flange distortion.

7.3 TC-SP3-W4X13

TC-SP3 was a W4X13 column tested at a temperature of 500^{o}C. Figure 5 shows the time-temperature response of the column. SP3 was heated to a temperature of 500^{o}C under a constant axial load of 10 kips. The temperature was maintained while an axial load was applied slowly at a rate of 4 kips/min as seen in Figure 6. Figure 7 shows a similar lateral displacement response to loading as SP2. The column reached a maximum axial load of 171.3 kips at failure.

7.4 TC-SP4 and SP5 – W4X13

TC-SP4 and TC-SP5 were both heated to 600^{o}C. The time temperature responses can be seen in Figure 5, where the heated column was held steady at 600^{o}C while the exterior columns remain near ambient temperature. The time-temperature response for TC-SP5 shows an anomaly in the constant heating rate of the column. This was due to a controller error discovered after 10 minutes that was heating the column at a rate that was faster than desired. Figure 7 shows the structural response of the column. The lateral displacement increases linearly over the duration of constant heating due to thermal expansion under an axially restraining load. The lateral displacements at mid-height of the exterior columns are smaller in comparison to a test of a lower temperature. This is because there is a significant drop-off in column strength and stiffness at 600^{o}C than at 500^{o}C or 350^{o}C. Both TC-SP4 and TC-SP5 failed by flexural buckling in the minor axis. The specimens failed at maximum axial loads of 120.3 kips and 120.9 kips for TC-SP4 and TC-SP5 respectively.

7.5 TC-SP6 – W4X13

SP6 was tested at a temperature of 350^{o}C. The resulting structural response shows that the stability of the heated column had a greater effect on the exterior columns than the previous tests at higher temperature. The residual strength of the heated column was greater in this test. Due to this material effect, the exterior columns began buckling simultaneously with the heated column. The exterior column lateral displacements were observed to be greatest in this test as compared to the other tests in this experimental program. The time-temperature response for TC-SP6 was disrupted due to programing error that increased the rate of heating of the heater controllers. The error was located quickly and the column temperature was allowed to level out for approximately one half-hour before reintroducing heat into the system. The error occurred at a temperature of approximately 100^{o}C and is assumed to have no effect on the outcome of this test. Column stability failure occurred at an axial load of 164.8 kips. This particular continuous column failed at a smaller axial load than TC-SP3 which was heated to 500^{o}C.

8. Mechanical Properties

Steel tensile tests were conducted on representative samples of the web and flange plates. Because all of the steel was produced in the same heat, only one set of tests were conducted on W4X13 and W5X16 respectively. The representative steel was taken from the ends of the continuous column

where the steel was under the lowest heating. The tensile testing was carried out by Laboratory Testing Inc. in Hatfield, PA. Table 2 summarizes the results of the material tests.

Table 2. Mechanical properties of steel at ambient temperature

Gr. 50 Steel	W4X13		W5X16	
	Web	Flange	Web	Flange
Yield (0.2%) Strength (ksi)	68.0	56.0	57.0	42.8
Tensile Strength (ksi)	83.0	74.5	71.0	69.5
Elongation in 2 in. (%)	22.0	31.0	36.0	41.0

The steel used in all tests is A992 steel with a nominal yield strength of 50 ksi.

9. Finite Element Analysis

Column buckling simulations were conducted using the 3D finite element method (FEM) modeling software ABAQUS (v6.12-2). Each column was modeled using four-node reduced integration shell (S4R) elements. Residual stresses in the steel section as well as geometric imperfections are included in the model. The modeling techniques can be found in more detail by Agarwal (2011) and are omitted for brevity. The magnitude of the geometric imperfections at mid-height of the column was modeled to be L/1000. The continuous column model consisted of a static RIKS analysis. This follows that the column was first heated before loading the specimen to failure. Thermocouple data was used to model the realistic steel surface temperatures present during the tests. Representative thermocouple data was taken from TC-SP3, TC-SP4 and TC-SP6 for use in structural models at 500ºC, 600ºC and 350ºC respectively. A parametric study similar to Agarwal and Varma (2011) was created to compare simply supported single columns and continuous columns over a range of slenderness values from 10 to 150. This study was completed to compare the models with the proposed equation and with experimental results of the W4X13 continuous column tests.

Eurocode-3 (EC3 2005) temperature dependent stress-strain (σ-ε-T) and thermal expansion (α-T) steel material models were used to model the thermal-mechanical strength behavior of steel. Actual steel strengths as obtained through material testing were used as the ambient yield strengths for the web and flange respectively.

10. Boundary Conditions and Restraints

The boundary conditions specified in the model were done so with intent to best represent the realistic boundary conditions found in the experimental setup. The half-cylindrical external supports provide free rotation in the lateral (minor) direction of the column while preventing rotation in the opposing direction and torsion. In the test, 1/4 inch plates were welded to the ends of the specimen to allow the bearing to be attached. For this reason, the cross section is restrained with a solid tie constraint to prevent changes in the cross section geometry. Similarly, the internal support cross sections are constrained to prevent out of plane deformations that would not be possible in the roller mechanism. The internal supports are modeled as rollers allowing rotation as well as axial displacement.

11. Model Results

The parametric study contains continuous and single columns modeled at temperatures that have been tested for the W4X13 cross-section. The slenderness ratios for these columns have been modeled within the range of 10 to 150. A slenderness ratio of 48 was chosen specifically to correspond with the actual slenderness found in the experimental portion.

Table 3. Continuous column FEM results

Temperature	Axial Load Capacity (kips)						
(^{o}C)	λ=10	20	48	60	80	100	150
20	257.1	242.3	199.3	188.8	148.1	97.6	44.2
350	249.0	234.2	191.3	159.5	114.4	83.7	40.9
500	218.9	214.6	164.8	134.5	97.7	71.2	36.1
600	179.9	175.0	120.4	103.0	73.9	53.8	27.4

Table 4. Single column FEM results

Temperature	Axial Load Capacity (kips)						
(^{o}C)	λ=10	20	48	60	80	100	150
20	257.1	242.3	199.3	188.8	148.1	97.6	44.2
350	247.6	217.6	174.4	130.2	89.3	70.5	34.1
500	209.5	190.0	107.9	86.6	62.2	43.4	21.2
600	128.5	109.0	62.8	51.1	38.0	26.7	13.9

Table 5. Ratio of continuous column FEM results to single column FEM results

Temperature	Ratio of continuous to single						
(^{o}C)	λ=10	20	48	60	80	100	150
350	1.01	1.08	1.10	1.23	1.28	1.19	1.20
500	1.04	1.13	1.53	1.55	1.57	1.64	1.70
600	1.40	1.60	1.92	2.01	1.95	2.01	1.97

The findings from the parametric study on W4X13 columns show that in all cases continuous columns fail at higher loads than comparable single columns. Table 3 and Table 4 show the results of the models using the software ABAQUS. The axial strength of the columns at elevated temperature is highest at 350^{o}C and slenderness ratio of 10. The axial strength decreases as temperature increases from ambient to 600^{o}C and also decreases as slenderness increases from 10 - 150.

Table 5 shows the ratios of the axial load capacity of continuous columns (given in Table 3) with respect to the axial load capacity of the corresponding simply supported column (given in Table 4). Table 5 shows that axial load capacity of continuous columns with intermediate span heated and cooler end spans is typically much higher than the axial load capacity of the corresponding simply supported column. As expected, the increase in the axial load capacity of the continuous column is dependent on the heated temperature as well as the slenderness ratio.

Table 6 shows the ratio of the axial load capacity calculated using the Equations proposed by Agarwal and Varma (2011) with respect to the axial load capacity predicted by the finite element analysis of the continuous columns given in Table 3. In most cases, the axial load capacity calculated using the proposed Equations is conservative with respect to the finite element results. The general trend is that the calculated axial load capacity is more conservative at higher temperatures and lower slenderness values.

Table 6. Ratio of the axial load capacity calculated by proposed equation and FEM results

Temperature	Ratio of calculated capacity to FEM results						
(^{o}C)	λ=10	20	48	60	80	100	150
350	0.74	0.78	0.70	0.73	0.81	0.89	1.03
500	0.64	0.65	0.68	0.73	0.82	0.92	1.08
600	0.49	0.50	0.62	0.64	0.74	0.84	1.03

Table 7 shows the ratio of axial load capacity calculated using the recommended Eurocode effective length reduction factor of 0.5. As shown in the Table, at lower temperatures, this methodology could potentially sacrifice safety by over-predicting axial load capacity of columns with slenderness greater than 80.

Table 7. Ratio of the axial load capacity calculated by Eurocode slenderness reduction and FEM results

Temperature	Ratio of calculated capacity to FEM results						
(^{o}C)	10	20	48	60	80	100	150
350	0.79	0.78	0.79	0.88	1.07	1.27	1.84
500	0.69	0.66	0.71	0.80	0.96	1.14	1.60
600	0.53	0.51	0.61	0.66	0.80	0.96	1.34

Figure 9 shows the design curves for the W4X13 column heated to 350 ^{o}C. It includes: (i) the design curve predicted for simply supported column by AISC 360-10, (ii) the design curve predicted for continuous column using AISC 360-10 and the proposed equation for estimated effective slenderness, and (iii) the design curve predicted for continuous column using Eurocode recommended effective length factor of 0.5L. The test result from TC-SP6 is also plotted in Figure 9 to illustrate the adequacy of the proposed equation. This test was chosen to show that in the range of lower temperatures (300-500^{o}C), the Eurocode recommended effective length factor may be unsafe. In this example, the 0.5L assumption predicts an axial load capacity that is greater than the experimental results. In comparison, the proposed equation matches very closely to the experimental results. The Figure also illustrates the experimental data point on the continuous column curve, and shows how this data point translates accurately to the single column curve when the effective slenderness (from the proposed equation) is used. This further illustrates how the effective slenderness works in shifting or relating the continuous and single column design curves adequately.

12. Conclusions

A series of laboratory-scale continuous column fire tests were conducted to investigate the thermal behavior of steel columns with rotational restraints due to continuity at each end. The tests were

conducted on steel columns that were continuous over three equal spans; the intermediate span was subjected to heating (steady-state thermal condition) and axial loading up to buckling failure.

The test results indicated that:

- Rotational restraints due to the continuous cooler columns can provide substantial increase in axial load capacity. The effective slenderness of the column in the intermediate (heated) span decreases with increasing temperature.
- The Equations proposed by Agarwal and Varma (2011) provide reasonable estimates of the effective slenderness and axial load capacity of the heated column with rotational restraints. These Equations provide more appropriate estimates than the constant assumptions of 0.5L or 0.7L suggested by Eurocode.
- Experimental results show good agreement with the proposed Equations to calculate effective slenderness of continuous columns at elevated temperatures.
- Finite element results indicate that the proposed Equations are better at predicting the axial load capacity of continuous columns over wide range of temperature and slenderness values.

The findings in this paper are limited to the parameters considered in the experiments and numerical models. Additional testing should be considered on steel shapes more common in building construction to supplement the parametric study presented herein.

Acknowledgements

The authors would like to acknowledge the National Science Foundation, and AISC and AISI for their continued financial support. The authors would also like to acknowledge the contributions of Dr. Anil Agarwal and Dr. Lisa Choe for their support and encouragement.

References

ABAQUS (2012). *ABAQUS/Standard Version 6.12 User's Manuals: Volume I-III*. Hibbitt, Karlsson, and Sorenson Inc., Pawtucket, RI.

Agarwal, A., and Varma, A. H. (2011). "Design of steel columns at elevated temperatures due to fire: Effects of rotational restraints." *Engineering Journal*, AISC, Vol. 48, No. 4, 4th Quarter, pp. 297-314.

Agarwal, A. (2011). "Stability Behavior of Steel Building Structures in Fire Conditions." Ph.D. dissertation, School of Civil Engineering, Purdue Univ., West Lafayette, IN.

Ali, F. and O'Connor, D. (2001). "Structural performance of rotationally restrained steel columns in fire." *Fire Safety Journal*, Vol. 36, No. 7, pp. 679-691.

AISC (2011). Manual of Steel Construction, Load and Resistance Factor Design, 14th Edition, American Institute of Steel Construction.

CEN (2005). *Eurocode 3: Design of Steel Structures, Part 1.2, Structural Fire Design*. European Committee for Standardization, Brussels, Belgium.

Choe, L. (2011). "Structural Mechanics and Behavior of Steel Members under Fire Loading." Ph.D. Dissertation, School of Civil Engineering, Purdue Univ., West Lafayette, IN.

Valente, J.C., Neves, I.C. (1999). "Fire resistance of steel columns with elastically restrained axial elongation and bending." *Journal of Constructional Steel Research*, Vol. 52, No.3, pp.319-331.

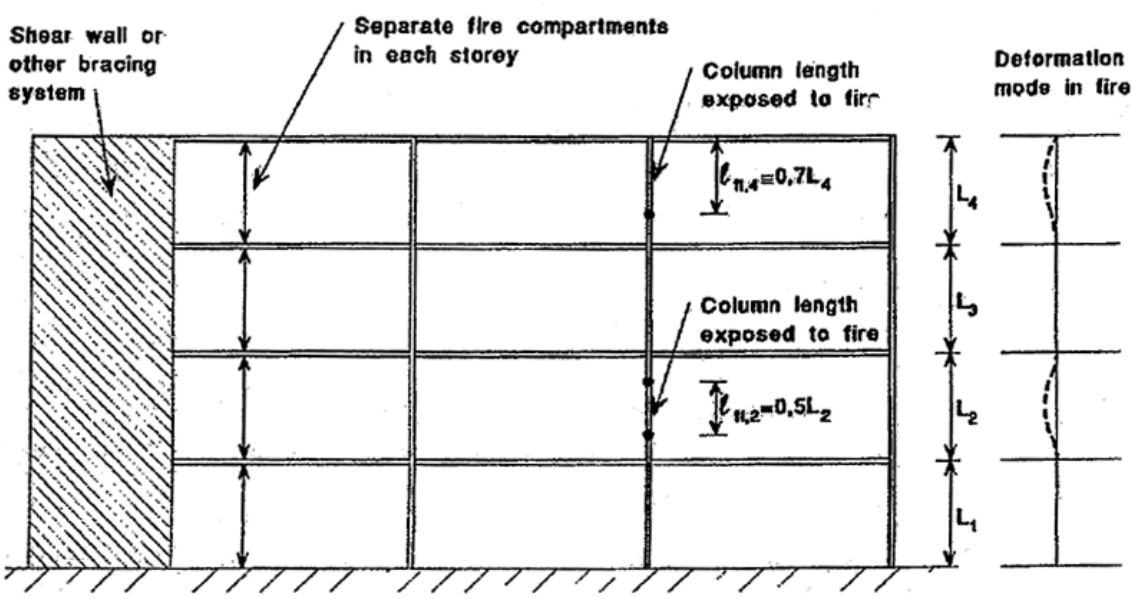

Figure 1 Buckling lengths of columns in braced frame (CEN 2005. Eurocode 3: Design of Steel Structures, Part 1.2, Structural Fire Design,
European Committee for Standardization, Brussels, Belgium.)

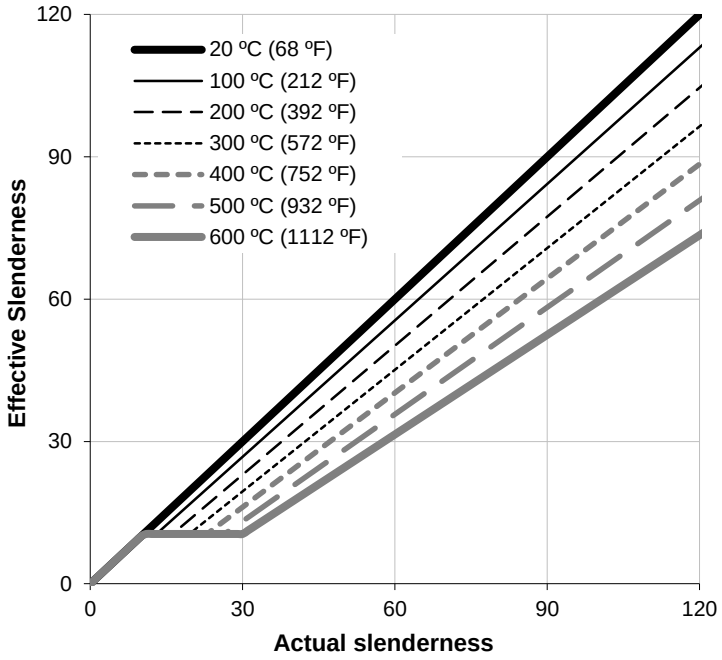

Figure 2 Proposed relationship between effective slenderness of continuous columns and the actual slenderness, Agarwal et al. (2011)

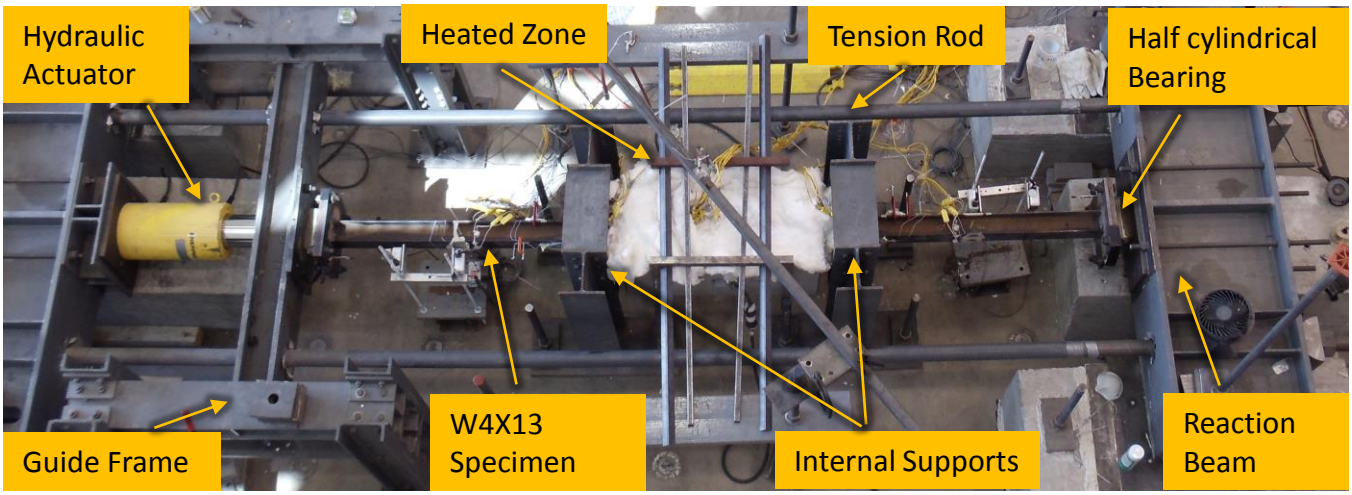

Figure 3 Top view of column test frame

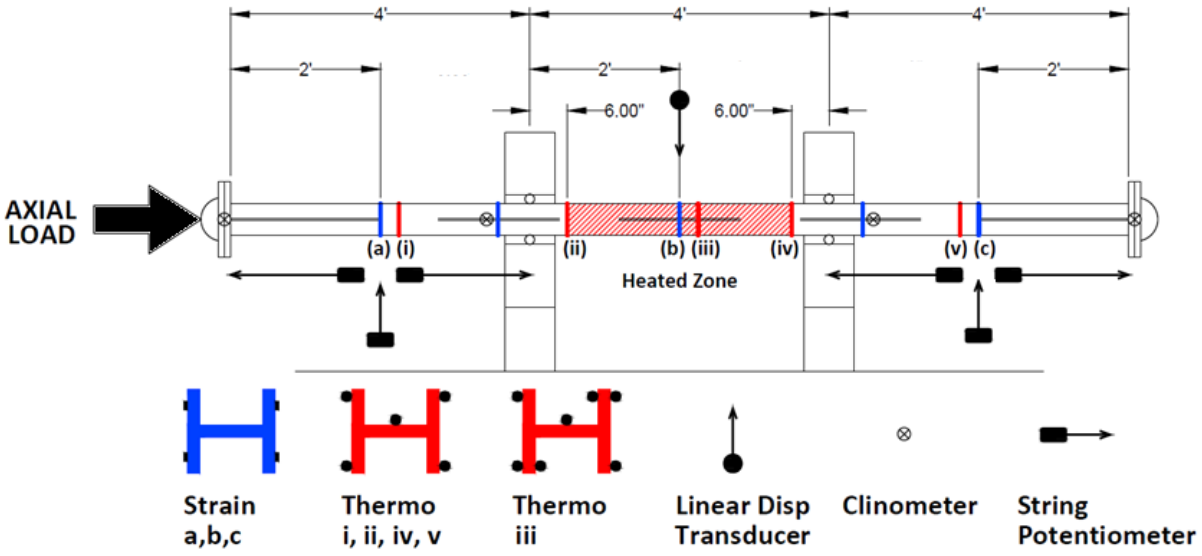

Figure 4 Instrumentation layout and specimen dimensions.

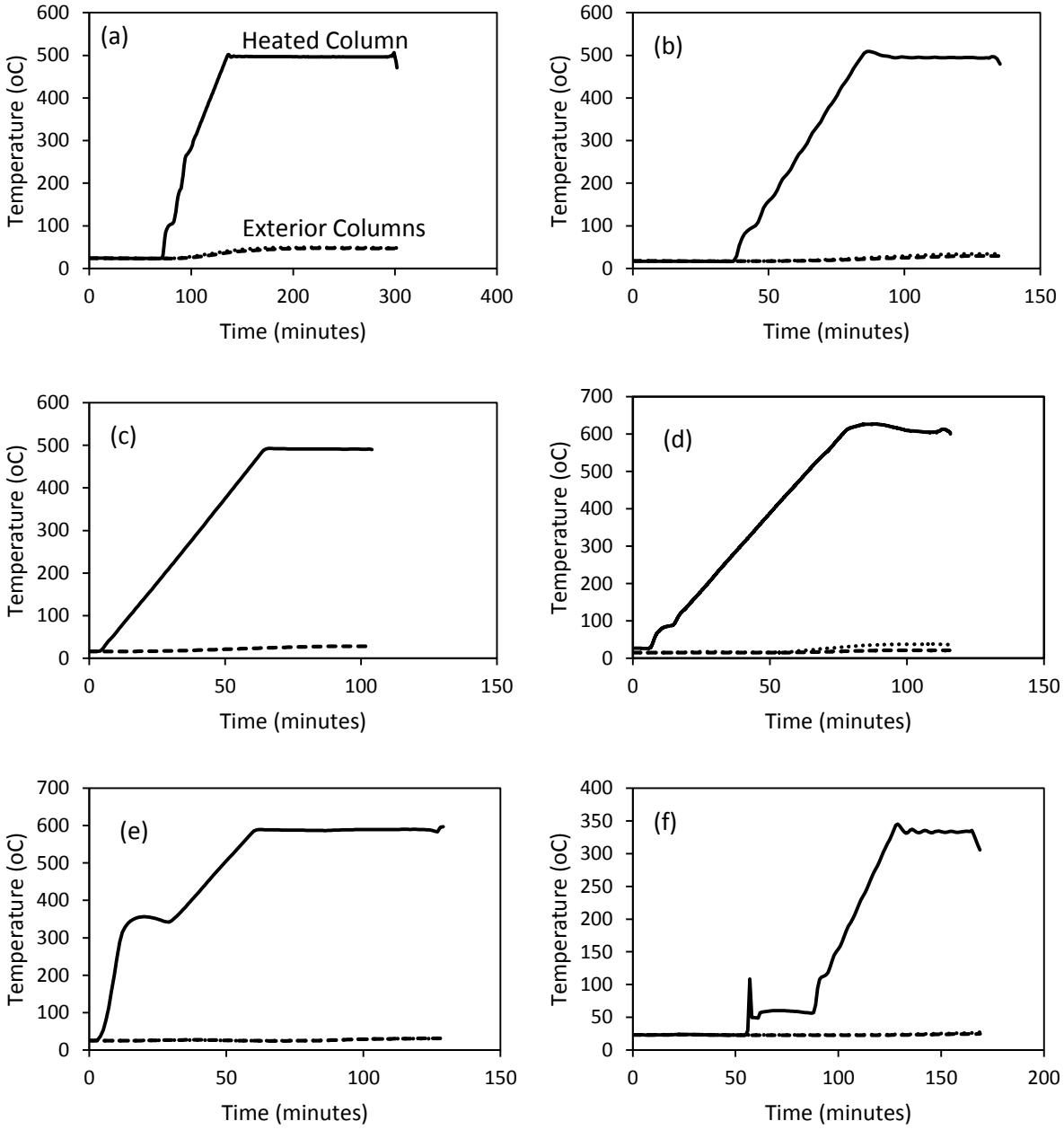

Figure 5 Time-Temperature Response of heated column and exterior columns for (a - f) TC-SP1 to TC-SP6.

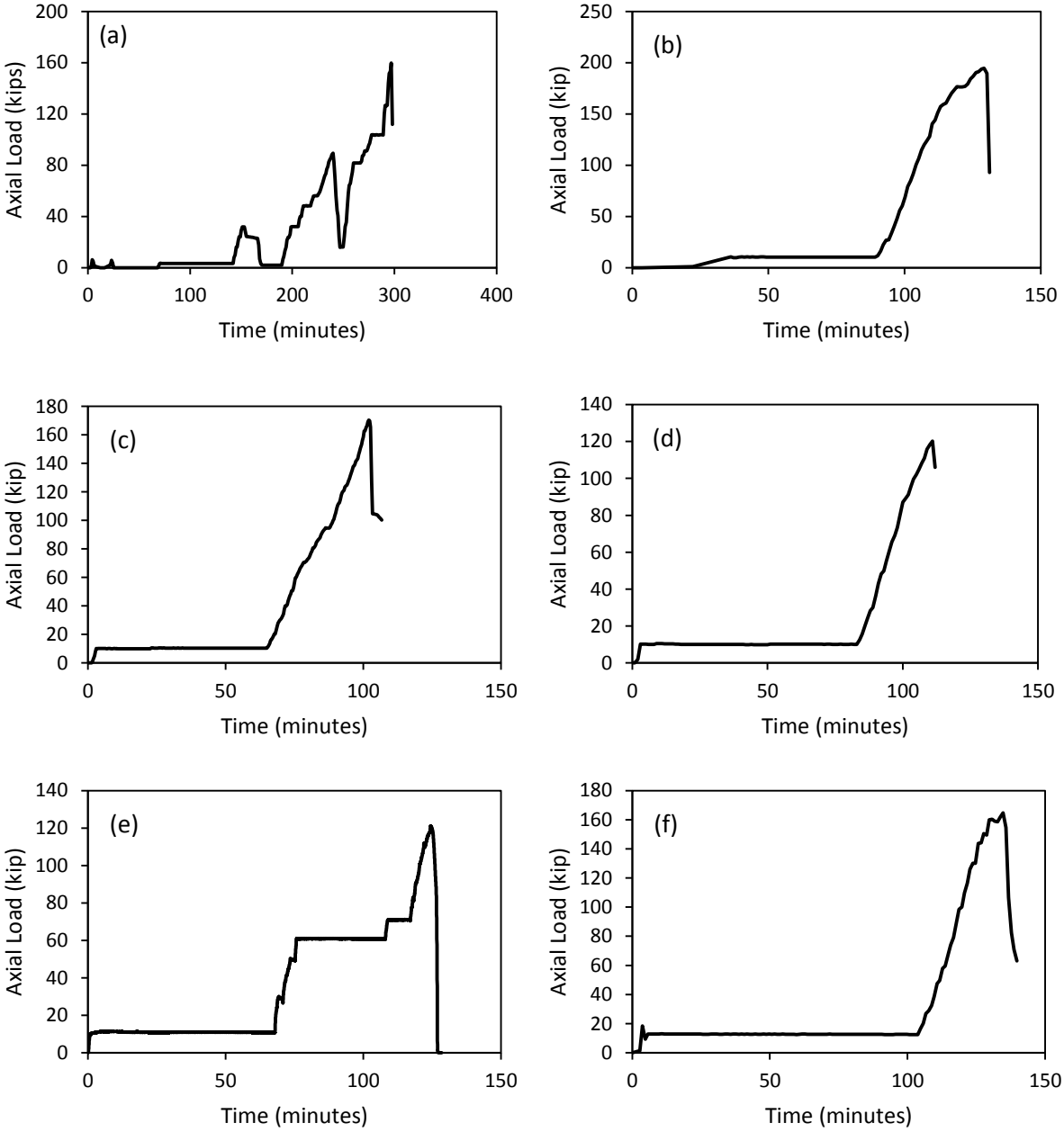

Figure 6 Mechanical load history of specimen (a - f) TC-SP1 to TC-SP6.

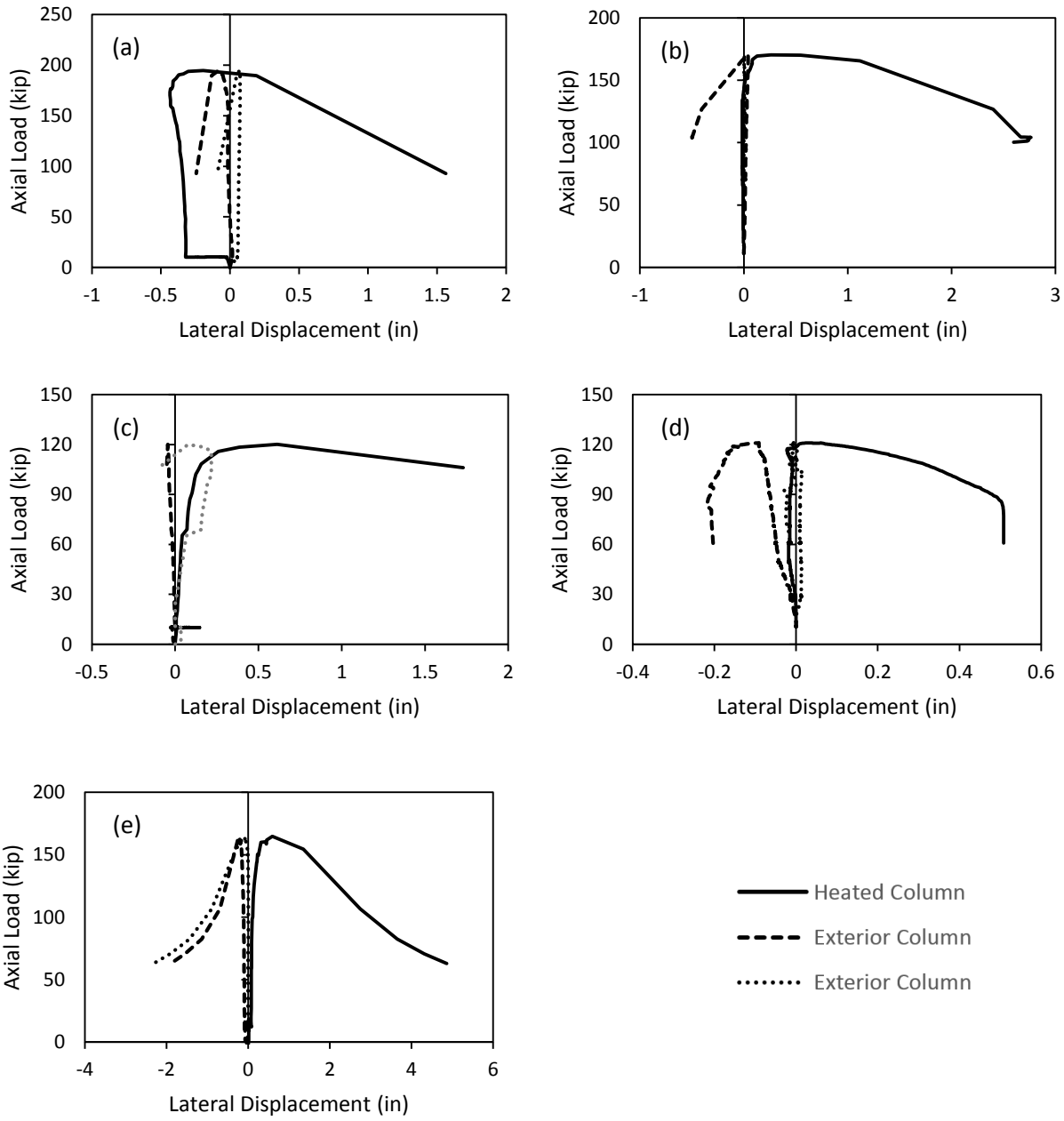

Figure 7 Lateral displacement response to combined heating and axial load for (a-e) TC-SP2 to TC-SP6

(a)

(b)

(c)

Figure 8 Final W4X13 continuous column deflected shape for (a) T=350°C, (b) T=500°C, (c) T=600°C

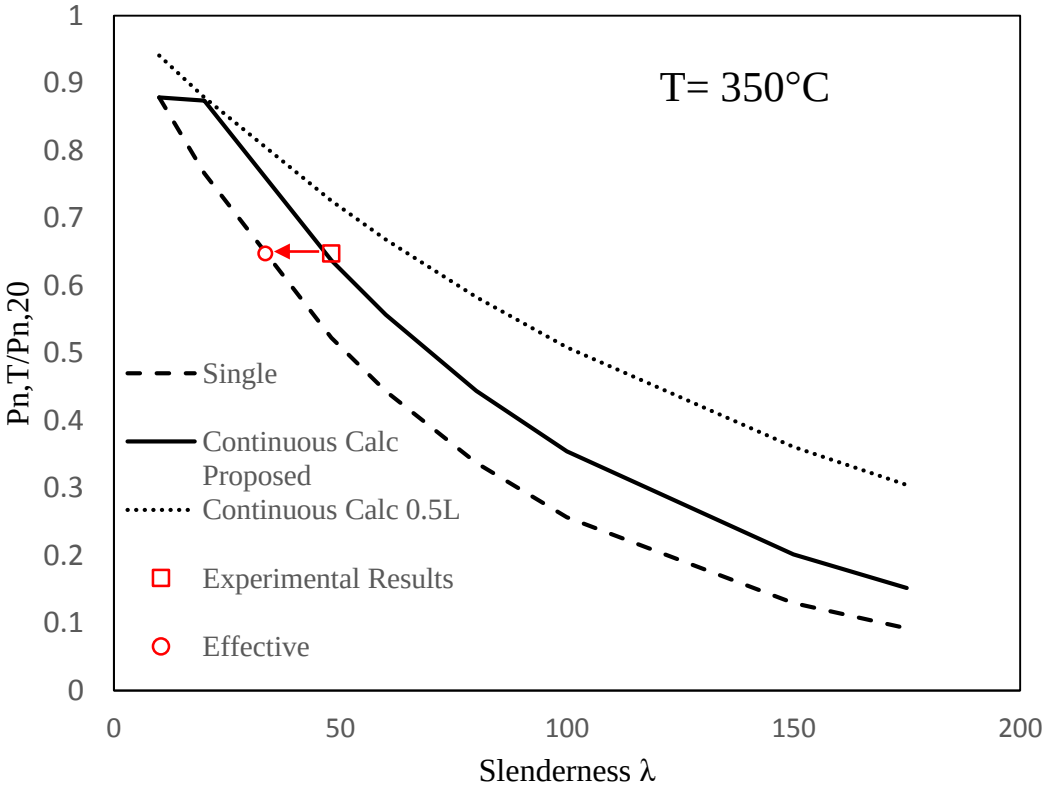

Figure 9 Continuous column capacity curves and test results at 350°C